PRE-PROCESSING AND SEMIVARIOGRAM ANALYSIS OF RADARSAT FINE MODE IMAGES FOR FOREST APPLICATION: TAPAJÓS NATIONAL FOREST, BRAZILIAN AMAZON

Silvana Amaral, Yosio E. Shimabukuro

Instituto Nacional de Pesquisas Espaciais - INPE
Caixa Postal 515, CEP 12227-010 São José dos Campos, SP, Brasil
telefone: 55 12 325 64 83, fax: 55 12 325 64 68
silvana@dpi.inpe.br, yosio@ltid.inpe.br

Frank J. Ahern , Joseé Levesque

Canada Centre for Remote Sensing - CCRS
588, Booth Street, Ottawa, K1A 0Y7, Ontario, Canada
Frank.Ahern@ccrs.emr.ca, Joseé.Valiquet @ccrs.emr.ca

ABSTRACT

This paper describes part of the activities developed in the PRORADAR (INPE/CCRS) evaluating the potentialities of RADARSAT images for forest application. The study site comprises the Tapajós National Forest, Pará State, Brazil. Two RADARSAT fine mode images were used: SGF- F2, acquired on May 20, 1996 and SGX-F5 acquired on May 05, 1996. In these images the relative image calibration and ortho-correction using geometrical modeling and the digital elevation model (DEM) were applied. The speckle filters (mediana, Lee and gamma) were tested over the images, considering different window sizes. Different forest types and land use classes were analyzed in the RADARSAT images: low plateau forest, two types of high plateau forest, disturbed forest, clearing and water. Since no significant difference between power average values for each class was observed, a semivariogram analyses were performed to evaluate its spatial variability. Although semivariograms varied according to the resampling procedure, they were considered an useful tool for discriminating land cover classes on RADARSAT images.

1. INTRODUCTION

The Brazilian Amazon, with approximately 3,370,000 km^2, requires remote sensing information to map and monitor its forest resources and the active processes that affect the land cover.

The frequent cloud cover over the Amazon region restricts the use of optical sensors for studying this region, then radar sensors are considered an alternative data source over this condition.

The radar data is a relative new technology and its potentialities are under of intense research. The pre-processing of RADARSAT images, including radiometric calibration and geometric correction, are under development.. Classification algorithms initially developed to optical sensors have to be modify to extract information from radar images, and they are not available in any image processing systems.

The analysis of radar images statistics, like the spatial correlation provides an important source of information to indicate possible classification criterious.

The objective of this paper is to present the pre-processing image procedure applied to two RADARSAT images and the analysis of semivariograms of forest and land cover classes distincted in the Tapajós National Forest region.

2. STUDY AREA

The study site comprises the Tapajós National Forest region, located in Santarém

city, Pará state, Brazil. It is limited by Tapajós River at west and BR-163 road at east and is located between the coordinates: 55° 30' and 54° 36' west Longitude and 2° 30' and 4° 18' south Latitude (figure 1).

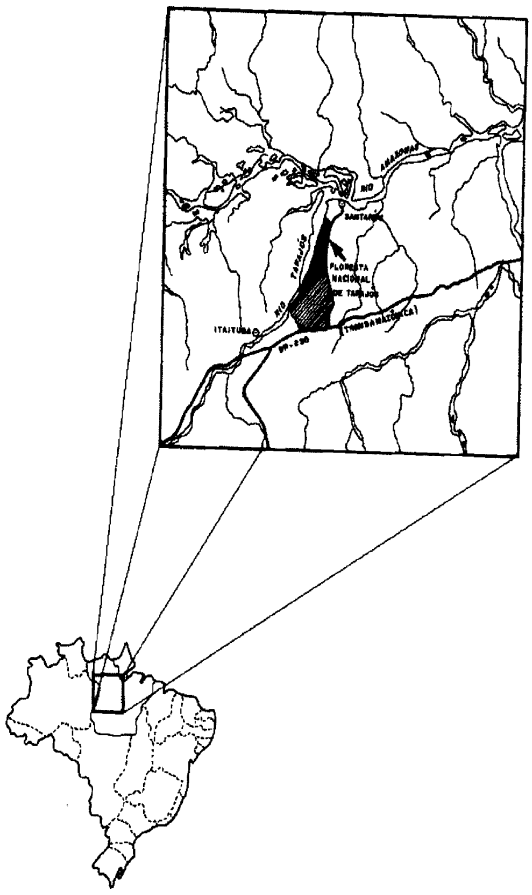

Figure 1. Study area - Tapajós National Forest

The region is characterized by the dry season (from August to November) and rainy season (from February to May). Temperature varies from 20°C to 35°C with the lowest maximum temperatures during the rainy season. (Hernandez Filho et al., 1993).

Two morpho-structural units characterizes the geomorphology of the region: the "Planalto Rebaixado da Amazonia", with altitude about 100 m, and the "Planalto Tapajós/Xingu" with altitude varying from 120 m to 170 m.

According to PROJETO RADAMBRASIL (1976), Tapajós National Forest vegetation types are based on the geomorphological description and can be divided in Amazonia Low Plateaus and Xingu and Tapajós High Plateaus. Tropical Dense Forest dominates both regions, with economic wood species more abundant at High Plateaus.

Tapajós National Forest is rich in trees of commercial value and is under a management program (Brazilian Institute of Renewable Resources - IBAMA) to explore these forest resources

Despite the conservancy nature of the National Forest, it has been disturbed for several factors. Some regions were explored by IBAMA as part of a management experiment and nowadays constitutes regeneration sites. Along Tapajós River and the road that communicates BR-163 to Tauari village there are several deforested areas due to human activities.

3. BACKGROUND

Semivariograms

A regional variable is defined by Matheron (1963) as a variable with a defined location in space. According to this definition, pixel values in a remote sensing image can be considered a regional variable, and its spatial variability can be express towards its semivariance.

Giving a transect of pixels in a remote sensing image, one can compute the digital numbers (DN) values difference considering pairs of pixels 1, 2, 3...n pixels far from each other. As the per-pixel variance is half of this values, the semivariance can be estimated by:

$$S^2 = 1/2\ [z(x) - z(x\text{-}h)]^2$$

where z(x) is the DN for pixels z and h is the distance between pixels (lag).

By averaging the number of pairs (m) separated by the same lag, then the average semivariance is:

$$\hat{S}^2 = 1/2m\ \ddot{a}\ [z(x_i) - z(x_i\text{-}h)]^2$$

The $\hat{S}^2$ is an unbiased estimate of the average semivariance of the population $\gamma(h)$. Higher $\hat{S}^2$ values mean less similarity between pixels.

Semivariograms displays the relation between the semivariance and the spatial separation (lag distances), describing the scale and pattern of spatial variability.

Some semivariograms examples are shown in figure 2, and they can be explained by lags intercepting the semivariance axis. It represents the spatially independent variance

and can be interpreted as consequence of either spatial randomness within the data set or due to microspatial variability at scale smaller than the minimum sampling resolution;

- C - spatial independent structural variance. It is given by sill minus nugget variance;
- h - lag - distance and direction in 2 or more directions between pairs;
- S - sill - maximum level of $\gamma(h)$;
- R - range - lag value at which $\gamma(h)$ no longer increases;
- N - nugget variance - value resulted by backwards extrapolation of the 2 first semivariance values.

Figure 2(a) presents a "classic" semivariogram, where $\gamma(h)$ values increases from 0 to a maximum (sill) and without variation after that. The nugget variance is illustrated in figure 2(b) and a semivariogram with no spatial auto-correlation in the data set is presented in figure 2(c).

A relatively large nugget indicates a micro-spatial variability having a large variance or a high level of spatial randomness (white noise) present in the data. Nugget value close to zero means that these influences are not distinguished in a data set. According to the spatial phenomenon nature and the sampling method adopted, it can or can not present the nugget effects.

The sill depends on the statistical variance of the data and the range depends on the spatial contiguity of the data.

Each spatial phenomenon has a semivariogram as an identity. The texture information since it is a lag function is present on the semivariogram. It describes how DN varies with the distance and can be used to classify different targets (Curran, 1988).

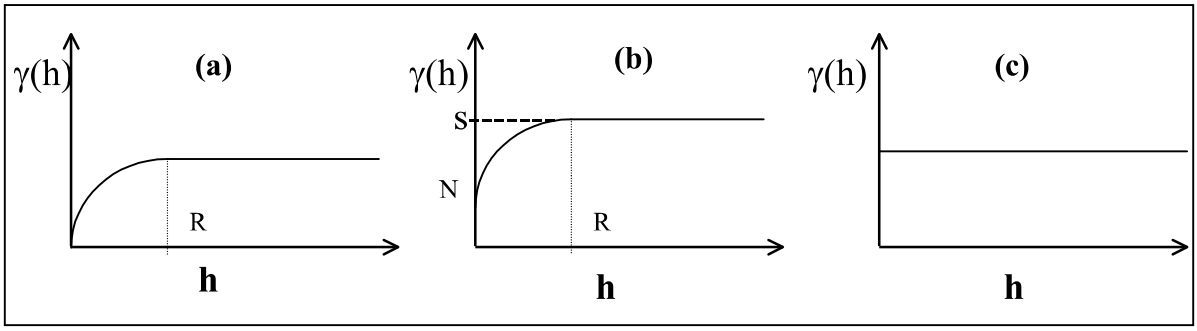

Figure 2 . Semivariograms through the origin (a), with nugget effect (b) and with no spatial autocorrelation (c).

4. DATA & METHODOLOGY

Image calibration and ortho-rectification

Two RADARSAT fine mode images, descending pass (D) were used in this work. The images characteristics are summarized in Table 1.

RADARSAT F2D and F5D images were first submitted to the relative radiometric calibration available at that time. It consisted basically on the elimination of the look up table applied at image recording process and the conversion of the magnitude digital numbers into power values (Shepherd et al., 1995).

Table 1 - RADARSAT images characteristics

	F5 - SGX	F2 - SGF
Acquisition Date	05/03/1996	05/20/1996
Mode	F5D - SGX	F2D - SGF
Incidence Angle (degrees)	45-48	39-42
Nominal Resolution (m)	10m (8.8 a 9.0m)	10m (8.8 a 9.0m)
Pixel Size (range, azimuth)	3.125 x 3.125	6.25 x 6.25
Central Latitude (degrees)	-3.07936	-2.91194
Central Longitude (degrees)	-54.96849	-43.83519
Pixels x Lines	12166x13766	6770x8100
Number of Looks	1	1

First, the bright values of the image was calculated by:

$\beta^{o}_{(R)} = 10 * \log_{10} [\{DN^2 + A_0\}/ A_{(R)}\}$ dB

where:

$\beta^{o}_{(R)}$ = brightness of ground range pixel (R)

DN = digital number

A_0 = the fixed offset

$A_{(R)}$= the look up table gain for the ground range pixel (R).

The gain and offset values can be found in the tape header and they were extracted during tape reading process.

Then, the sigma nought values (σ^{o}) could be obtained, correcting the brightness values for incident angle $I_{(R)}$, where I is a function of range r:

$\sigma^{o} = \beta^{o}_{(R)} + 10 * \log_{10} \{\sin I_{(R)}\}$ dB

This conversion is made assuming flat terrain and spherical earth geometry.

Finally, power digital numbers ($DN_{(P)}$) were obtained from the σ^{o} values from the relation: $\sigma^{o} = 10 \log_{10} DN_{(P)}$

After this process, the power image generated were submitted to an integrated and unified geometric modeling to correct the image geometry (Toutin, 1995). It corrects globally the image instead of locally as the polynomial model does and requires fewer ground control points. When compared to image registration procedure, it is less influenced by the GCP distribution.

The procedure adopted to RADARSAT ortho-correction is presented in figure 3.

First, RADARSAT image was read from the magnetic tape and the orbit file which contains the attitude, ephemeris, and view geometry information was extracted

Then, ground control points (GCPs) with X, Y and Z coordinates were acquired for the image, based on topographical maps at 1:100,000 scale. The geometric model was computed and the GCPs were modified to minimize the residuals mean square errors.

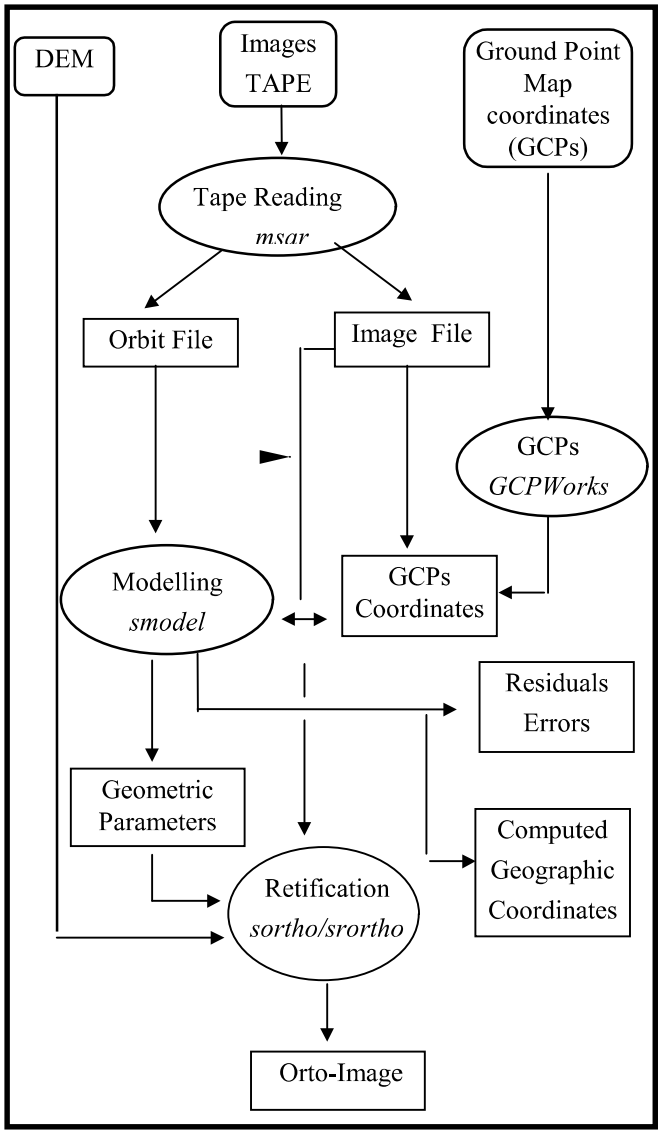

Figure 3. Ortho-rectification procedure.

Source: adapted from Toutin (1995).

The orbital parameters were first used to initialize the geometric model. In sequence, an interactive least-square adjustment was used to solve the equation of observations with GCPs. At least 7 GCPs are need to solve the equations for SAR images. The geometric model parameter, the residuals on the GCPs, the errors of the check points, and the computed cartographic coordinates for each point were resulted from this step.

Finally, the rectification to generate the ortho-image in the geometric projection system defined was performed. To obtain the ortho-image, a DEM were used to compute the elevation distortion for each image pixel.

The DEM was obtained from triangular irregular network grid of digitized isolines.

The mediana filter were used to resample the original image to 12.5m pixel spacing, generating an ortho-corrected and speckle filtered image.

Semivariogram Analysis

The semivariogram analysis was performed over samples extracted from RADARSAT images at different stages in the image pre-processing. The objective was to analyze the effect of each processing over the semivariogram of the classes and to suggest the better methodological approach.

The semivariograms were calculated over the magnitude image (16 bits), the power image radiometrically calibrated (32 bits), and after the geometrical correction (12.5m pixel spacing, 8 bits).

The class definition was based on the Phytoecological Map (1:400,000 - FUNATURA, 1991) based on PROJETO RADAMBRASIL (1976). Visual analyses of the differences of surface roughness observed in color composition presented on TM images, and the aerial photographs (scale 1:20,000), were used as ancillary data.

The following classes were defined to the semivariogram analysis:

(1) plain-forest - Dense tropical forest of sedimentary areas, waved relief, dissected plateau, with emergent trees;

(2) plateau-forest - Dense tropical forest of sedimentary areas, high plateau, with emergent trees + Open tropical forest with palm trees in the plateau;

(3) plateau-forest2 - Dense tropical forest of sediment areas, low and dissected plateau, with emergent trees and uniform arboreal cover;

(4) clearings - deforested areas at Tapajós National Forest surroundings;

(5) water - Tapajós river;

(6) disturbed forest - anthropogenic activities inside the National Forest.

Classes 5 and 6 were only available to the F5 image, since F2 image did not cover the same area.

For each class, one sample of 30 x 30 pixels were located over the images. This sample size was bigger than those used by Miranda and Carr (1994) and were restricted by the limitation of the semivariogram software used (Vario-win) .

The sample positions were used as a mask to extract digital values from the images. Then, they were added a header and line and column coordinates.

To the semivariograms analyses direction were equal to zero, angular tolerance equal to 90 and no limits to the maximum bandwidth, which means that omnidirectional variogram were calculated. From the analysis of the semivariograms it was chosen the processed image that provided the best class distinction to modeling. Sill, range and nugget values were estimated to describe the variogram of each class.

5. RESULTS

Pre-processing

RADARSAT-SGF-F2 image after relative radiometric calibration is presented in figure 4. The noisy aspect of image requires a speckle filtering for any further application.

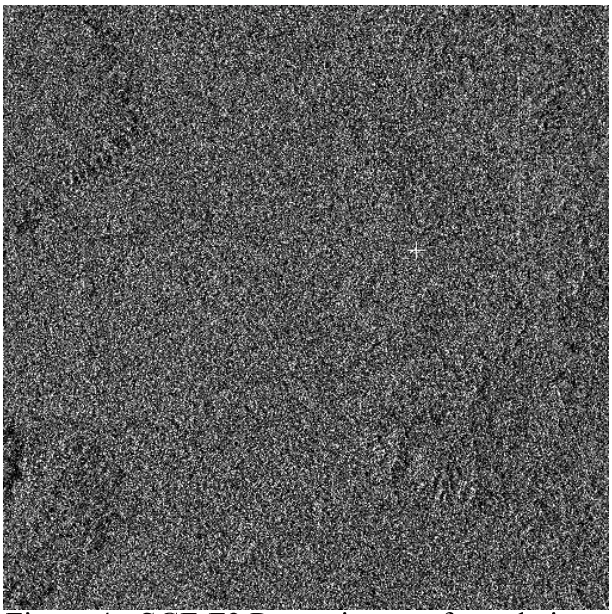

Figure 4 - SGF-F2 Power image after relative calibration

The gamma filter using a 9x9 window size presented the best result when visually comparing Lee and Gamma filter using different window sizes (3x3, 5x5, 7x7, 9x9). However, some saturated pixels can be observed (figure 5). These pixels correspond

to power values higher than 1, that was attributed to saturation during the recording process of the image, and to terrain variations like double-bounce effects from relief. This is confirmed when saturated pixels remained in the image even after a mediana filter, 11x11 window size.

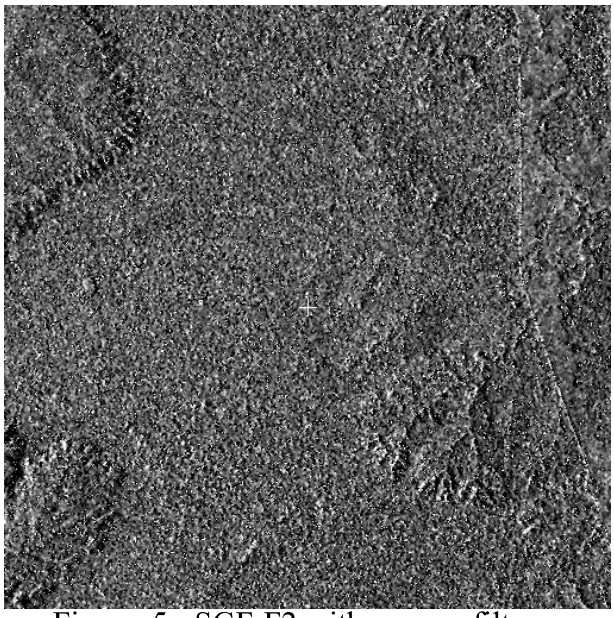

Figure 5 - SGF-F2 with gamma filter.

Figures 6 and 7 present RADARSAT F2 and F5 images respectively, after ortho-correction.

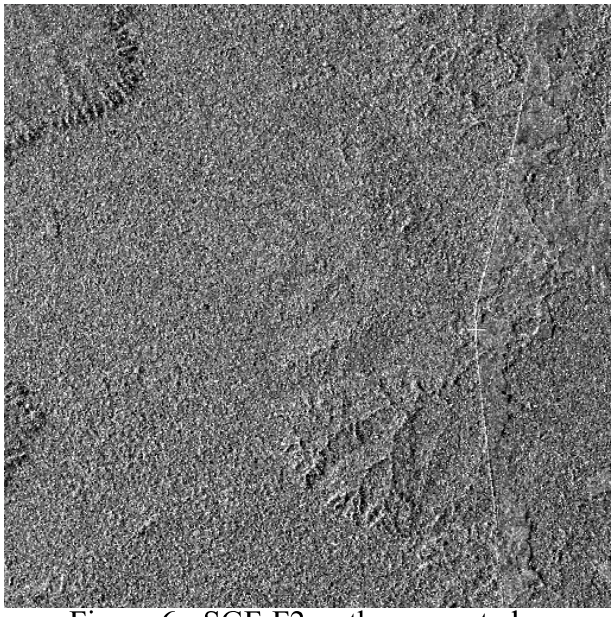

Figure 6 - SGF-F2 ortho-corrected.

The mean square residuals computed for F2 and F5 were 37 m and 29 m respectively. A mediana filter were used to the ortho-correction resampling procedure. This way, the original power image were corrected resulting in a 12.5m pixel spacing image. Mediana filter was selected because it was the less effective filter, among the available ones in changing image statistics. Other filters could mask the image texture for the semivariogram analysis.

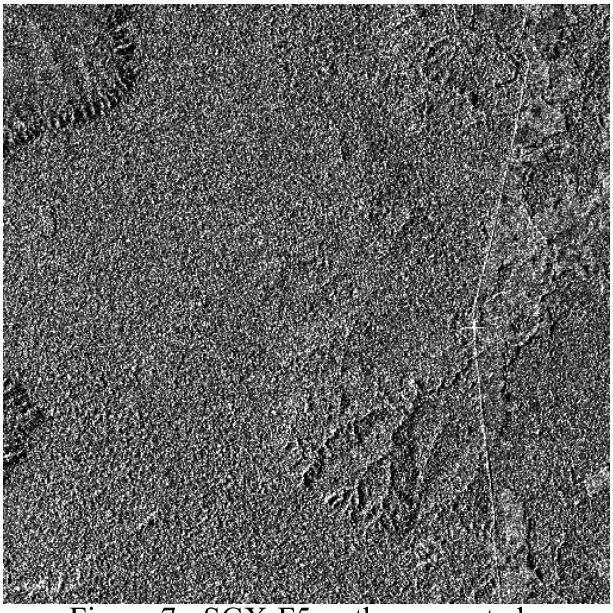

Figure 7 - SGX-F5, ortho-corrected

Considering a visual analysis, the images basically discriminated forest in the plateau, forest in the plain, gaps inside the forest, deforested areas, the drainage pattern and the main road. There was no observed difference between forest types.

Canopy roughness and double-bouncing effect are more evident at F5 image than in F2 image, because of the higher incident angle. This suggests that F5 image is more suitable to define boundaries between forest and deforested areas.

Semivariograms

Table 2 presents the average and the variance for each sample acquired over power image used to the semivariogram analysis. The average values were very close to each other and the variance always contains the other class average value.

For F5 power image, water presented the lowest variance and it was the single class that could be distinct from the others by its average and variance. Plateau-forest and plateau-forest2 presented almost the same average and variance values. Disturbed forest class presented the highest variance

and contains all other forest average and variances.

Table 2 - F5 and F2 average and variance power values for the analyzed classes

	F5-SGX - Power		F2-SGF - Power	
	average	variance	average	variance
clearing	0.186	0.064	0.164	0.028
Plateau-F	0.179	0.066	0.211	0.070
PlateauF2	0.172	0.043	0.181	0.053
Planicie-F	0.130	0.028	0.183	0.055
Disturb-F	0.222	0.082	-	-
Water	0.004	1.27E-05	-	-

For F2 image, plateau-forest class presented higher variance, containing all of the others classes. Clearing class presented the lowest variance.

These values emphasized that it would be impossible to distinct these classes only considering the pixels values. Some measurement that would take into account the spatial arrangement of the pixels has to be used in order to distinct classes.

The semivariance analysis provided a description of the spatial variation of the pixel values and presented a distinct signature of each class. The legend of figures 8 to 13 are related to the forest classes described before: (C) clearing; (PT2) plateau-forest2; (PF) plain forest; (PT) plateau forest; (W) water; (DF) disturbed forest.

The first semivariogram is related to F2 - Amplitude image (figure 8), where a strong nugget effect can be observed for all plotted classes. As nugget effect can be related to micro-spatial variability with a large variance, or high level of spatial randomness, it could be attributed to speckle.

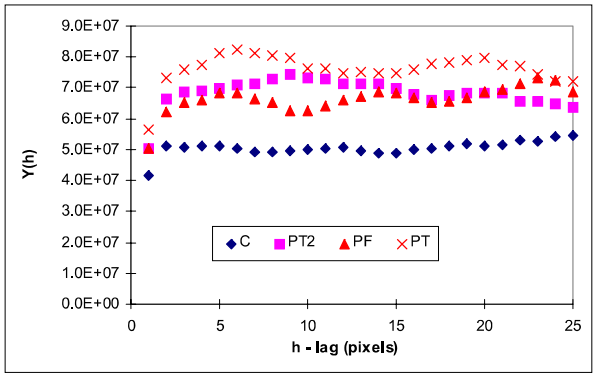

Figure 8- F2 Amplitude image semivariograms

Plateau forest and plain forest classes presented cyclical semivariograms, plateau-forest2 semivariogram was confused with plateau forest and plain forest. Clearing class presented a typical spherical semivariogram, with a sill value distinct from the others.

After F2 image were converted to power values with relative radiometric calibration, the semivariograms shapes remained the same for each class (figure 9), the nugget effect is still present, and the semivariance values (X axis) had its scale changed because data were converted from 16 bits - amplitude values to 32 bits - power values. At this scale, plateau forest were better distinct from the others, as well as clearing class.

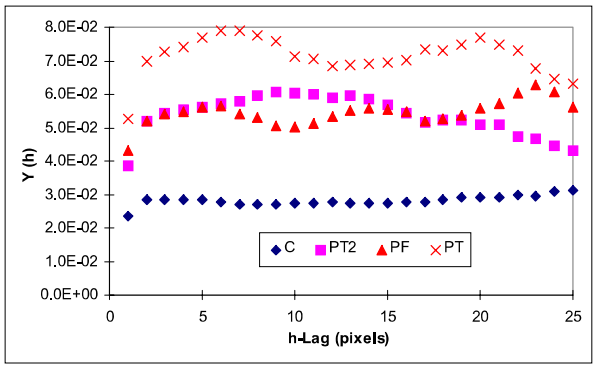

Figure 9- F2 power image semivariograms

F2 image was resampled to 12.5m pixel size and 8 bits image using a mediana filter during the ortho-correction process. As the image was scaled from 32 to 8 bits, the semivariance of the sample and the scale changed (figure 10). The semivariograms shapes were smoothed and the nugget effect was reduced probably because of the speckle reduction.

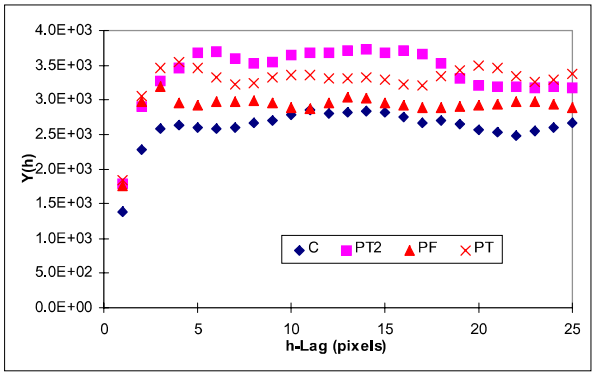

Figure 10- F2 ortho-correct image semivariograms.

However, it is interesting to point out that plateau-forest2 presented the higher sill value, opposite to it had been observed in the previous semivariograms. This can be attributed to the scaling process (32 to 8 bits).

F5 amplitude image semivariogram did not present any nugget effect (figure 11). Water class semivariogram was completely null, indicating that no spatial auto-correlation occurred in the sample, due to the water specular backscattering. Forest class semivariograms were mixed indicating some confusion between its semivariance signatures.

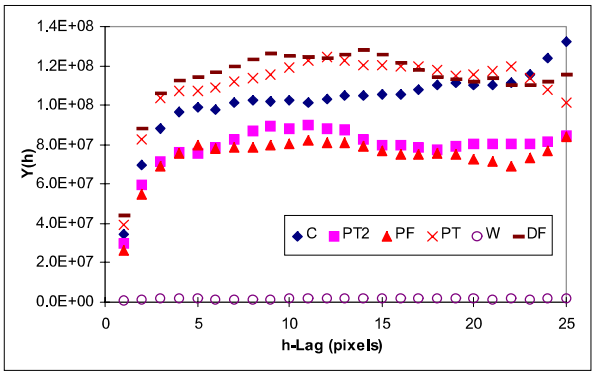

Figure 11 - F5 amplitude image semivariograms

After the relative radiometric calibration the signatures became more distinct (figure 12). Disturbed forest presented the highest sill value, with cyclical variation, probably due to the complex nature of this class, with different contribution of soil and vegetation. Clearing class presents a spherical semivariogram like observed in F2 samples.

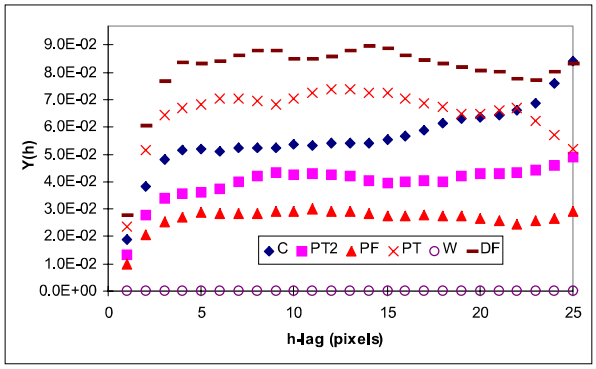

Figure 12- F5 power image semivariograms.

After geometric correction, with resampling and scaling of the image, the class variances increased (figure 13). Class semivariograms were closer to each other than they were at power image. Plateau forest and plateau forest2 presented similar semivariogram with lower range value (around 2 lags). Clearing could be distinguished by its range value (about 7 lags) and plain forest by its lowest sill value.

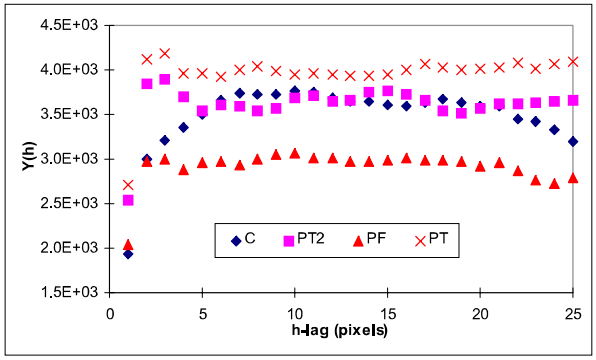

Figure 13 - F5 ortho-correct image semivariograms.

Class semivariogram varied according to pre-processing image type. F2 and F5 power image presented the better semivariogram configuration and were used to estimate their descriptive parameters.

Table 3 presents the range (R), sill (S) and nugget (N) values obtained from class semivariograms of F2 and F5 power image.

For F2 image, clearing, plateau forest and plateau forest2 could be discriminated by their range values and plateau forest could be distinguished by its sill value.

For F5 image disturbed forest could be distinguished by its range values and the other classes by their sill values.

Table 3 - Semivariograms parameters of F2 and F5 power image

	F2-SGF - Power			F5-SGX - Power		
	R	S	N	R	S	N
C	2.3	0.016	0.0126	3.12	0.053	-
PT	3.08	0.06	0.0168	3.12	0.069	-
PT2	6.47	0.033	0.0264	3.64	0.033	0.006
PF	3.36	0.029	0.0264	3.90	0.028	-
W	-	-	-	3.38	0.085	-
DF	-	-	-	2.50	1.315	-

Miranda et al. (1996) obtained similar results from semivariogram analysis, working with JERS-1 images over northwestern Brazil and different land cover, including open, dense and flooded vegetation.

6. CONCLUSIONS

RADARSAT F2D and F5D images pre-processing procedure was described. The images with relative radiometric correction and ortho-correction using a digital elevation model were presented.

Ground Control points acquired during the field work are going to be introduced in the ortho-correction procedure. This will improve the image position precision and it will enable the correlation between image backscattering and biophysical forest measurements.

Semivariograms analysis can discriminate forest types and land cover even if the classes are not visually distinguished on the image, as was observed with the class plateau forest2. Power image provided the best dispersion of the classes at the semivariograms.

These results suggested that it would be possible to classify F2 and F5 power image using its semivariograms.

Because of the nature of C-band, RADARSAT images present information from the vegetation superior stratum. Field work information, related to trees height and dispersion, were extracted for the two principal forest types presented in the area. This information are going to be compared with F2 and F5 power values to analyze the influence of canopy structure over the images.

8. ACKNOWLEDGMENTS

This research is part of the PRORADAR project between INPE and CCRS. The authors would like to thank Canadian International Development Agency for the financial support.

9. REFERENCES

Curran, P.J. 1988. The Semivariogram in Remote Sensing: An Introduction. Remote Sensing of Environment 24: 493-507.

Hernandez Filho et al., 1993. Relatório Final: Projeto de Inventário Florestal na Floresta Nacional do Tapajós. Projeto de Cooperação Técnica desenvolvido pelo INPE/IBAMA/FUNATURA/IITO, INPE, São José dos Campos (INPE-5423-PRP-171).

Matheron, G. 1963. Principles of geoestatistics. Econ. Geol. 58:1246-1266.

Miranda, F.P., Carr, J.R. 1994. Application of the Semivariogram Textural Classifier (STC) for Vegetation Discrimination Using SIR-B Data of the Guiana Shield, Nothwestern Brazil. Remote Sensing Reviews, vol. 10, pp. 155-168.

Miranda, F.P., Fonseca, L.E.N., Carr, J.R., Taranik, J.V. 1996. Analysis of JERS-1 (Fuyu-1) SAR data for vegetation discrimination in northwestern Brazil using the semivariogram Textural classifier (STC). International Journal of Remote Sensing, 17(17): 3523-3529.

PROJETO RADAMBRASIL. Folha S/A 21 - Santarém. Rio de Janeiro, DNPM 1976. (Levantamento dos Recursos Naturais, v.10).

RADARSAT International, 1995. RADARSAT-Illuminated - Your guide to products and services.

Shepherd, N.W. and Associates., 1995. CDPF Output Data Calibration. Technical Note No. 4.2.

Toutin, T. 1995. Multisource data fusion with an integrated and unified geometric

modeling. EARSil Advances in Remote Sensing. Vol. 4, N2 - X., p. 118-129.